CAMFlow-3 Flow Controller and Hall Thruster Testing

IEPC 2024-499

Presented at the 37th International Electric Propulsion Conference
P. Baudis Convention Center, Toulouse, France
June 23-28, 2024

Curtis A. Woodruff [1], Magdalena Parta [2], Ryan Fox [3], David L. Carroll [4]
CU Aerospace (CUA), Champaign, IL 61822

Leanne Su [5], Tate Gill [5], Christopher Sercel [5], William Hurley [5], Parker Roberts [5], Madison Allen [5], Jon Van Noord [6], and Benjamin Jorns [7]
University of Michigan, Ann Arbor, MI 48109

Abstract: **The Cycle Automated Mass Flow (CAMFlow) system is a compact, reliable, and well-regulated flow control unit for electric propulsion systems. CAMFlow uses a control scheme that enables stable operation using fixed frequency valve openings with variable duration (Boolean valve states), even for the low flow rates necessary for sub-kilowatt Hall effect thrusters. This methodology removes system complexity, places the onus of reliability on valve cycle life, and combined with the fixed operational frequency, allows for a direct correlation between system life and valve cycle life. Through the use of inexpensive space-rated components, CAMFlow technology provides a reliable low-cost flow controller that is well-suited for sub-kilowatt Hall/ion thrusters. The CAMFlow control scheme was successfully implemented in a TRL 6 xenon flow controller (XFC) integrated with a pressure management assembly (PMA) system and tested and validated on a 600-Watt Hall thruster in the Large Vacuum Test Facility at the University of Michigan. This testing included open loop, closed loop, and cold start operations. Further, two Lee Co. valves were cycled > 114 million cycles demonstrating long-life potential of the XFC, and two higher pressure Lee Co. valves were cycled > 56,000 cycles demonstrating long-life potential of the PMA. This equates to 300 kg Xenon throughput, or 300% life (i.e., 200% margin) on 100 kg throughput. CAMFlow-3 underwent vibrational and thermal vacuum testing; its performance was the same before and after the environmental testing. The stainless steel CAMFlow-3 unit has a mass of 2.78 kg and a volume envelope of 1,530 cm^3 (note that the mass could be reduced to ~1.9 kg if titanium was utilized instead of stainless). Thermal modeling was supported by nominal operating test results. The technology is broadly applicable over a larger range of flow rates for a broader commercial market. The system was designed and fabricated with size, functionality, risk tolerance, and cost considerations appropriate for NASA Class-C/D missions.**

I. Introduction

There are a number of sub-kilowatt Hall effect thrusters that have been or are currently under development [Levchenko, 2018; Lemmer, 2017]. Domestic, higher TRL concepts include Busek's BHT-200 and BHT-600 systems [Hruby, 2019], NASA Glenn Research Center's Sub-Kilowatt Electric Propulsion (SKEP) thruster [Schmidt, 2018; Kamhawi, 2019], and NASA Jet Propulsion Laboratory's Magnetically Shielded Miniature (MaSMi)

[1] Director of Propulsion, woodruff@cuaerospace.com, AIAA Member.
[2] Senior Engineer, magda@cuaerospace.com, AIAA Member.
[3] Staff Engineer, fox@cuaerospace.com, AIAA Member.
[4] President, carroll@cuaerospace.com, AIAA Fellow.
[5] Graduate Research Assistant, AIAA Student Member.
[6] Lead Engineer in Research, Space Sciences Research Laboratory, noord@umich.edu, AIAA Member.
[7] Associate Professor, bjorns@umich.edu, AIAA Associate Fellow.

Copyright © by the authors. Published by the Electric Rocket Propulsion Society with permission.

thruster [Conversano, 2017a; Conversano, 2019]. Operationally, these thrusters typically employ xenon as a propellant with discharge voltages ranging from 200-300 V and currents from 0 – 5 A. Given the Hall thruster rule of thumb that that 1 A of discharge current corresponds to 1 mg/s flow of xenon propellant through the anode, these voltage and power requirements translate to the flow range identified in this solicitation, i.e., 0-5 mg/s. An additional 7-10% of this anode must be supplied to the electron source for the device, the cathode. In terms of total propellant throughout, i.e., lifetime, mission studies for small-scale, class-D missions have shown that 500 kg class missions could require as much as 100 kg of propellant over lifetimes extending 20 khrs [Conversano, 2017b]. Similarly, the number of cycles on the system (for start-up and shut-down) can be >10,000.

These flow and lifetime requirements must be coupled with other system considerations. Examples include the limits on inlet and outlet pressure, the flow control accuracy, mass and power requirements, and fault tolerance. With the acceleration of commercial launches for satellites having Hall and ion thrusters, reliable low-cost options for the xenon flow controller (XFC) and propellant management assembly (PMA) modules are demanded. Relevant requirements are listed for VACCO's XFC module in Cardin *et al.* [Cardin, 2013]. To supplement the qualification standards desired in the development of this XFC, we also include fault tolerance required informed by Class-D mission requirements as well as specifications for the XFC currently under development for the 13 kW Hall thruster system under development for the NASA-sponsored Advanced Electric Propulsion System (AEPS) [Jackson, 2017]. The µFCU from German company AST [Harman, 2013] uses a pulsed valve with a tortuous path to control flow down to the 0-5 mg/s level with a valve similar to the VACCO valve. Key differences are the control scheme and valve pulse rate, and the CUA system strives to increase valve life with lower frequency operation. The µFCU valves claim an impressive 300 million operational cycles, so even at higher pulse rate they can enable a large quantity of propellant throughput. Maxar is working with Moog [Lenguito, 2019] on an extended range of operation XFC using a proportional flow control valve (PFCV) and includes a latching valve that can switch between two cathode flow fractions, but PFCVs are susceptible to more failure modes over many cycles than the Lee Co. valves used in CUA's CAMFlow system.

The CU Aerospace (CUA) Cycle Automated Mass Flow (CAMFlow) project evolved to include both XFC and PMA capabilities [Woodruff, 2022; Woodruff, 2024], regulating all the way down from bottle pressure to the hall thruster. While the units could be offered separately, the system as designed integrates both together, with a shared control electronics board. Note that CAMFlow is readily adapted to have additional flow line splits to enable switching between different cathode flow fractions (as done for the CAMFlow-2 unit [Woodruff, 2022].

II. CAMFlow-3 Design and Fabrication

CAMFlow uses an innovative control scheme that enables stable operation using fixed frequency valve openings with variable duration (Boolean valve states), even for the low flow rates necessary for sub-kilowatt Hall effect thrusters [Woodruff, 2022]. This methodology replaces system complexity, places the onus of reliability on valve cycle life, and combined with the fixed operational frequency, allows for a direct correlation between system life and valve cycle life. Through the use of inexpensive space-rated components, CAMFlow technology provides a reliable low-cost flow controller that is well-suited for sub-kilowatt Hall/ion thrusters. The all-welded CAMFlow-3 hardware includes 37 laser welds (15 in the PMA and 22 in the XFC) for system integrity and is shown in **Figure 1**.

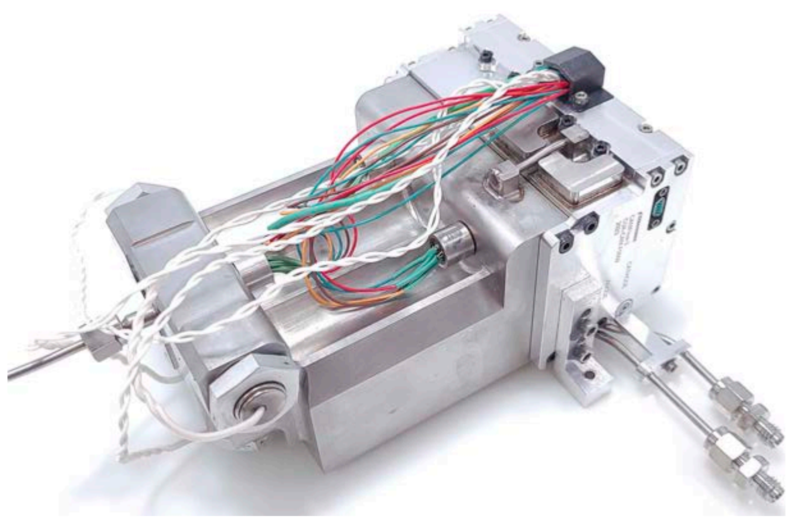

Fig. 1: CUA's CAMFlow-3 system. Cycle Automated Mass Flow (CAMFlow) technology provides reliably stable gas flow rate to sub-kiloWatt Hall thrusters. The body of the compact CAMFlow-3 system with PMA+XFC, enclosed electronics, and valving is approximately 1.5-liters in volume.

Figure 2 shows the flow path diagram for the combined XFC-PMA system. The design generally follows that of the previously reported CAMFlow-2 system [Woodruff, 2022].

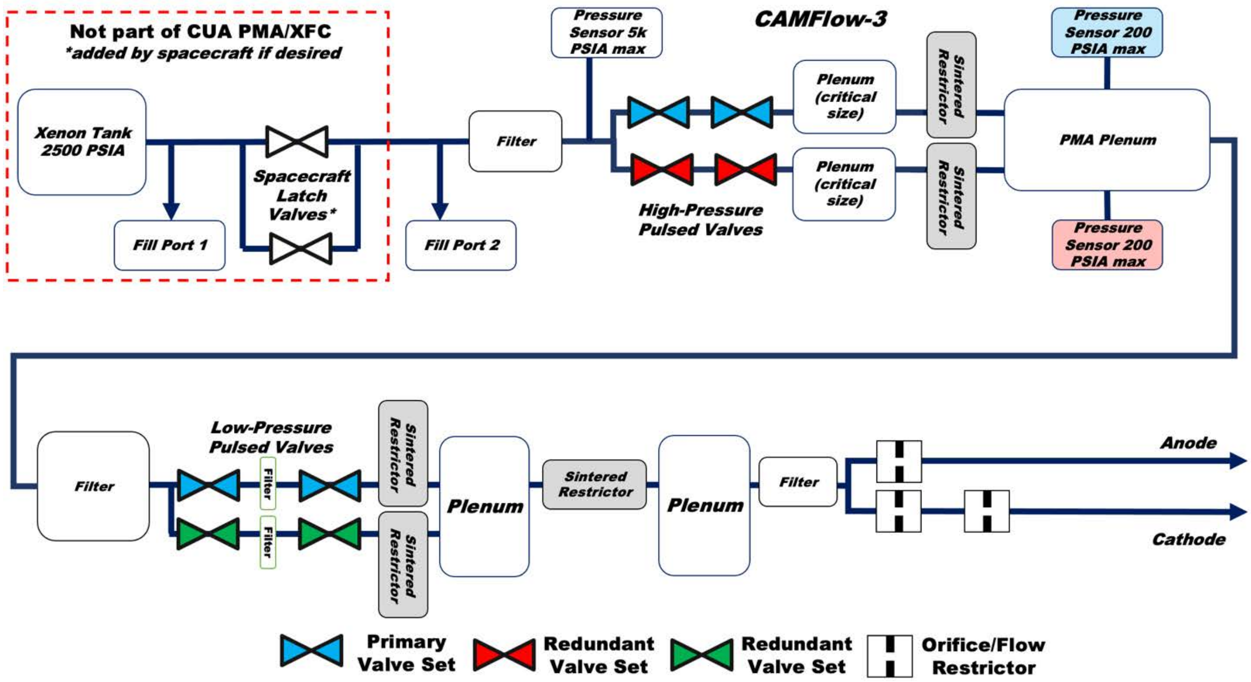

Figure 2. Flow path diagram for CAMFlow-3

The top portion of **Figure 2** comprises the PMA and the bottom portion of **Figure 2** the XFC. The PMA has series-parallel redundant valve sets and dual low-pressure sensors. The pressure in the PMA plenum is loosely regulated by filling to ~ 100 PSIA and allowing blowdown to ~30 PSIA. This operation requires a single cycle on the active set of PMA valves. By narrowing the pressure band, finer ultimate flow control is possible, but at the cost of system life. In the event an active valve is stuck closed, the secondary valve set can be used. A stuck open valve is more difficult to detect, but should not affect operation. Similarly, the pressure sensors are tied to their respective PMA valve chains, so if readings become anomalous, they can be swapped. Depending on the control electronics (2 versions) there exist some cases where there is only single fault tolerance, but most situations allow for dual fault tolerance.

The bottom section represents the XFC. This takes the low-pressure output from the PMA and regulates flow rate. By design, the XFC operates in a closed loop mode targeting hall thruster current. Open loop operation is possible, but the accuracy and consistency of this mode depends on external factors.

Note that CAMFlow supports a second XFC for a cathode cold start operation (e.g. for the MaSMi thruster [Conversano, 2017a; Conversano, 2019]), but it was not included in this build as the test unit did not require the feature. This would attach to the same place as the existing XFC portion.

Figures 3 and 4 show the external components of CAMFlow-3. Note the pressure sensors are small in relation to their cutouts. This is because flight heritage sensors are supported in addition to smaller, less expensive devices.

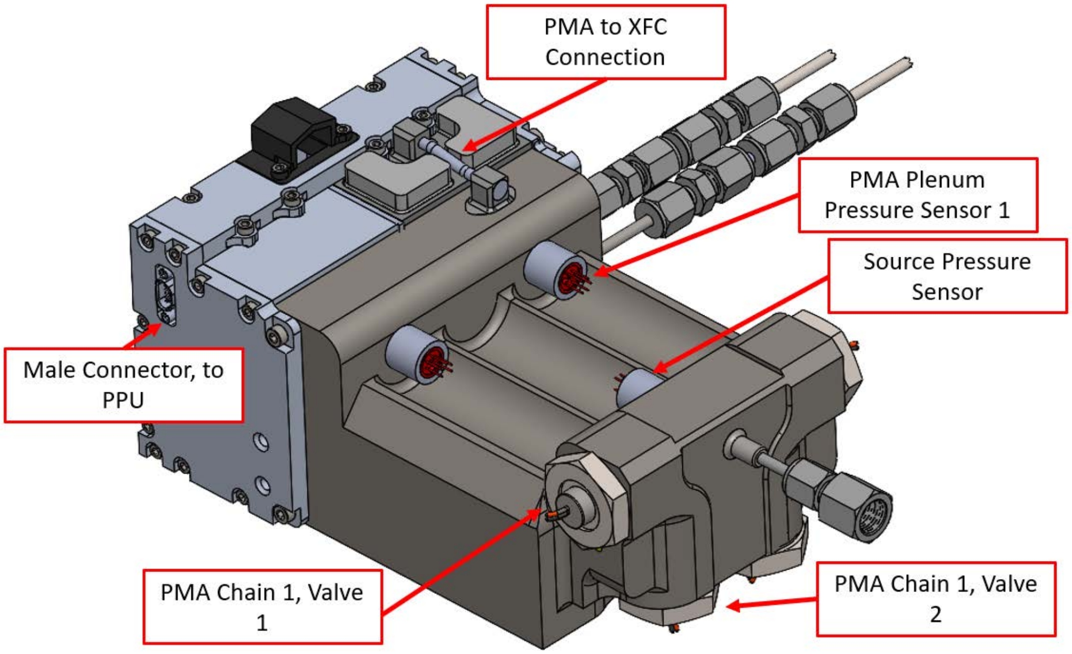

Figure 3. CAMFlow-3 features shown from the power processing unit (PPU) connector side.

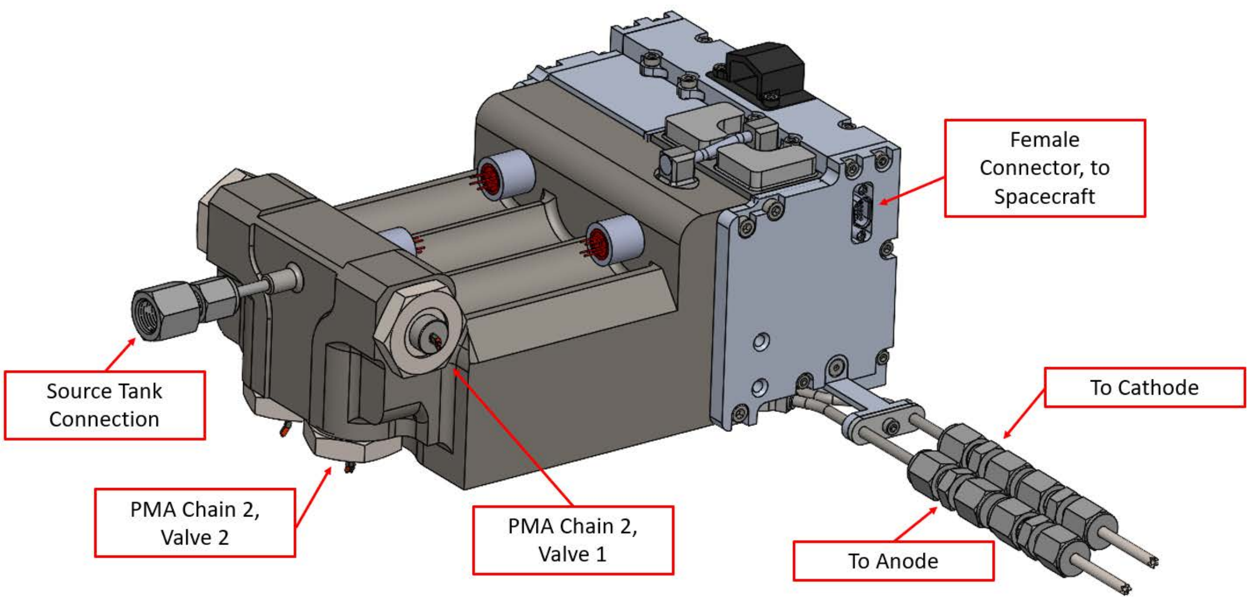

Figure 4. CAMFlow-3 features shown from the spacecraft connector side.

The CAD renders here show Swagelok fittings on the exits, although tube welding is preferred for a flight system. Further, the final flow balancing orifices for anode and cathode are externally attached in this version, allowing for systems to customizable long after the internal features are welded shut. **Figure 5** shows the exterior dimensions of CAMFlow-3 in inches. A photograph of the fabricated CAMFlow-3 hardware is shown in **Figure 1**.

The electronics boards are located between the XFCs and PMA behind cover plates. The XFC and PMA materials are all stainless steel while the brackets and cover plates are aluminum. Excluding the mounting brackets and extended tubing, the dimensions of the body are 80 mm (3.1 in) x 112 mm (4.4 in) x 173 mm (6.8 in), or approximately 1.55 liters for the entire package containing two XFCs and one PMA. System performance information is provided in **Table 1**.

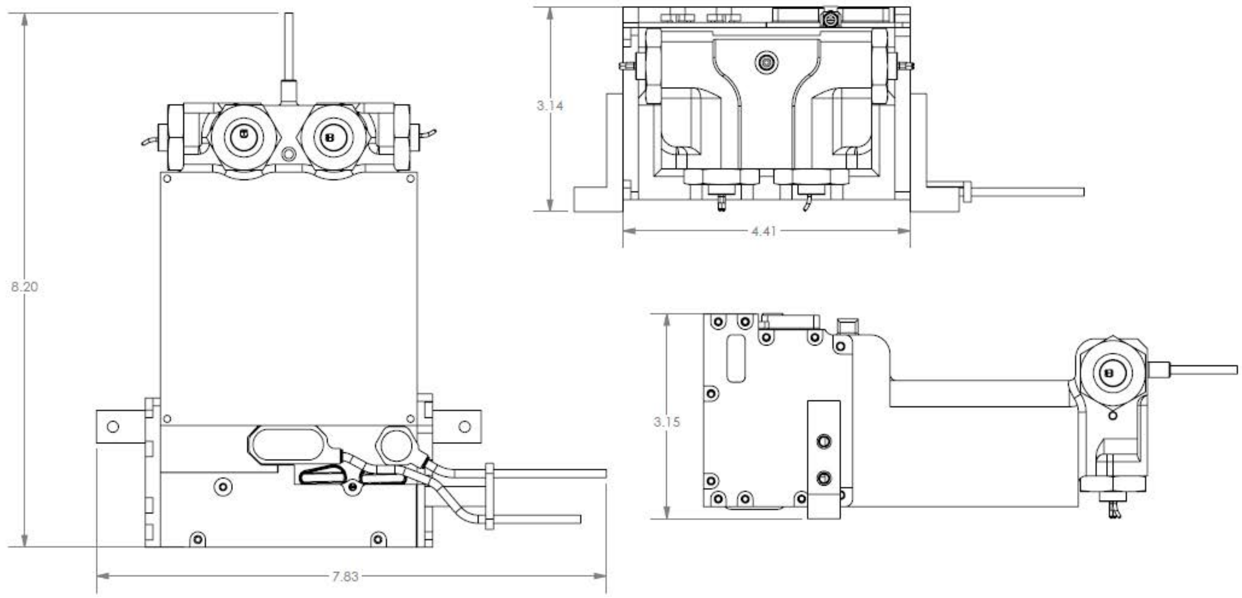

Figure 5. CAMFlow-3 exterior dimensions [units are inches].

Table 1. CAMFlow-3 performance information.

CAMFlow-3 Performance	PMA	XFC
Anode Flow Rate [mg/s]	0 – 15	0 – 15
Flow Split to Cathode (Customer Option)	N/A	0 – 15% w/ quick change option for different % split
Heaterless Cathode Start Flow Rate (Requires second XFC)	N/A	0 – 15% w/ quick change option for different % split
Flow Pressure Variation at Outlet [psia]	100 +20/–80	< 2%
On/Off Cycles	> 55,000	> 100 $x10^6$
Inlet Pressure [psia]	40 – 3500	30 – 100
Outlet Pressure [psia]	30 – 100	< 6
Total Throughput [kg]	300	300
Working Gases (others possible)	Xe, Kr	Xe, Kr
Gas Cleanliness – Inline Filter [μm]	10	10
Mass [kg]	2.1 (can be light weighted by switching from stainless to titanium)	0.66
Volume [liters]	1.1	0.4 (w/ PCBs)
Internal Leakage [scc/s of He]	$< 1x10^{-4}$	$< 1x10^{-4}$
External Leakage [scc/s of He]	$< 1x10^{-6}$	$< 1x10^{-6}$

Two versions of control electronics were developed for CAMFlow-3. The first system uses discrete timing and control logic without an onboard microcontroller. Analog voltages go into and out of the system, as well as GPIO pins for control. The timing and control parts are all available as space rated options, however size constraints mean that most switching components are careful-COTS. A male and female micro-Dsub connector are used for each connection to the unit. These connections allow for the spacecraft to monitor and enable the PMA, while providing the Hall thruster PPU the ability to regulate the XFC and maintain closed loop control. A microcontroller version was developed but not yet produced. It still requires power rails from the XFC to operate, but allows a single RS422 interface to control the entire system. These connections and a LabView interface used for control and testing of CAMFlow-3 are discussed further in [Woodruff, 2024].

Flow and valve life testing are described in [Woodruff, 2024]. Summarizing those results, valve life testing of the XFC valves exceeded 114 million cycles, and PMA valves exceeded 56,000 cycles, which equates to 300 kg Xenon throughput (or 200% margin on the original 100 kg goal for CAMFlow-3). With readily customizable flow balancing orifices, CAMFlow-3 can provide any anode / cathode ratio of flow, from a total flow of 0-15 mg/s Xenon.

III. Hall Thruster Testing with CAMFlow System

To demonstrate the ability of the CUA CAMFlow-1 XFC to operate a sub-kW class Hall thruster, the CAMFlow-1 system was sent to team partner UM to interface the developed XFC with a 600 W thruster. The experimental setup, telemetry, and results from this task are described below. The key technical objectives, which were accomplished over a week-long test campaign performed at UM, were designed to mirror the anticipated requirements for a flight like system:

1. Demonstrate XFC ability to command cold flow (thruster off) in open loop mode
2. Demonstrate ability to start thruster in open loop mode with XFC
3. Demonstrate thruster throttling with XFC in open loop mode: set flow manually in XFC software to adjust thruster current
4. Demonstrate thruster throttling with XFC in closed loop mode: set target discharge current in software and allow XFC to control to setpoint
5. Demonstrate "hard start" and shut down in closed loop mode

Large Vacuum Test Facility (LVTF)

UM employed the 6 m × 9 m Large Vacuum Test Facility (LVTF) for performing the thruster testing. It is cryogenically-pumped by 19 re-entrant helium pumps and capable of achieving an effective pumping speed of 550 kl/s on xenon and base pressure < 10^{-7} Torr. LVTF has been employed to test several forms of electric propulsion systems and basic plasma experiments over the past three decades. It is equipped with a flow manifold, break out box, power supplies, and optically-isolated telemetry system configured for operating and running Hall thrusters.

600 W Hall thruster

UM employed the 600-W class, BHT-600 Hall thruster built by Busek Co. for the systems level test. The University of Michigan owns a four-element array of BHT-600s (**Figure 6**) that were originally procured in 2005. Nominally, each thruster employs a barium oxide cathode, operates on xenon, and discharges at 200-400 V with powers ranging from 200 W to 800 W. This power range corresponds to flow rates from 0.6-4 mg/s. For this program, only one of these units was once operated and interfaced with the flow system.

Before the start of this effort, the BHT-600 cluster at UM was originally obtained in 2005 [Jorns, 2018] and had been in storage for over ten years. An initial check out test therefore was performed at UM in the first months while the XFC was being constructed at CUA. It was discovered through this test that all the cathodes in the cluster had poisoned during storage and were not recoverable. As a work around, a 20-A class laboratory LaB6 hollow cathode was substituted (**Figure 6**). The thruster was shown to operate stably over the throttling range with this cathode, and this configuration subsequently was adopted for the systems level test.

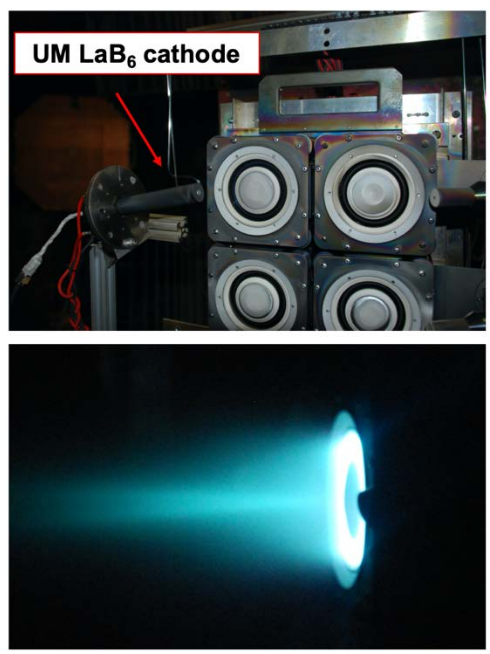

Figure 6: (Top) BHT-600 cluster at UM with the LaB6 cathode installed. (Bottom) thruster operating in UM vacuum facility.

Table 2 shows the thruster throttle points we employed for this investigation. The cathode flow fraction was 15% for all conditions. This generous split was necessitated by the fact that the replacement LaB6 cathode was not designed to operate at the standard 8% flow rate used when the thruster runs with its nominal cathode. We also note from this table that the flow rate and discharge current are linearly related. This is consistent with most state-of-the-art (SOA) Hall thrusters.

Table 2. BHT-600 throttling points in this test series. The cathode flow fraction was 15% for all conditions.

Voltage	Current [A]	Power [W]	Anode mass flow [mg/s]
300	2	600	2.53
300	2.2	660	2.67
300	2.5	750	2.98
300	1.8	540	2.23
300	1.5	450	1.88
200	3	600	3.4
200	3.3	660	3.67
200	3.8	760	3.95
200	2.7	540	3.11
200	2.2	440	2.58
400	1.5	600	1.69
400	1.7	680	2.15
400	1.9	760	2.38
400	1.3	520	1.53
400	1.1	440	1.50

Flow system

UM has a dedicated flow manifold that regulates high pressure (800 psi) xenon through commercial flow controllers to deliver gas to thruster test articles inside LVTF. For the integrated test, the laboratory flow controllers were bypassed, and the CUA flow controller was installed in series with one feed line to the CAMFlow PMA and the two CAMFlow XFC lines were then few to the anode and cathode (**Figure 7**); note that **Figure 7** shows that the volume of the CAMFlow unit is relatively small compared to BHT-600. Two pressure transducers were also installed on the anode and cathode lines immediately adjacent to the thruster.

Power supplies

The thruster was operated on laboratory power supplies located at UM. The discharge power supply consisted of a Magna-power electronics 60 kW system with a maximum output voltage of 1000 V. The power for the cathode heater, keeper, and electromagnets was provided by a series of TDK Lambda power supplies.

Telemetry system

Telemetry was monitored in two ways during the systems level test: through the UM in-house data-logger---an optically-isolated telemetry system---and with a control computer provided by CUA. The data reported here is from the CUA measurements. Key telemetry included the thruster discharge current, the flow rate, and the discharge current set points for the controller. **Figure 8** shows the I/O layout for the flow controller. The discharge current feedback was provided from a current shunt measurement located in the UM's facility breakout box.

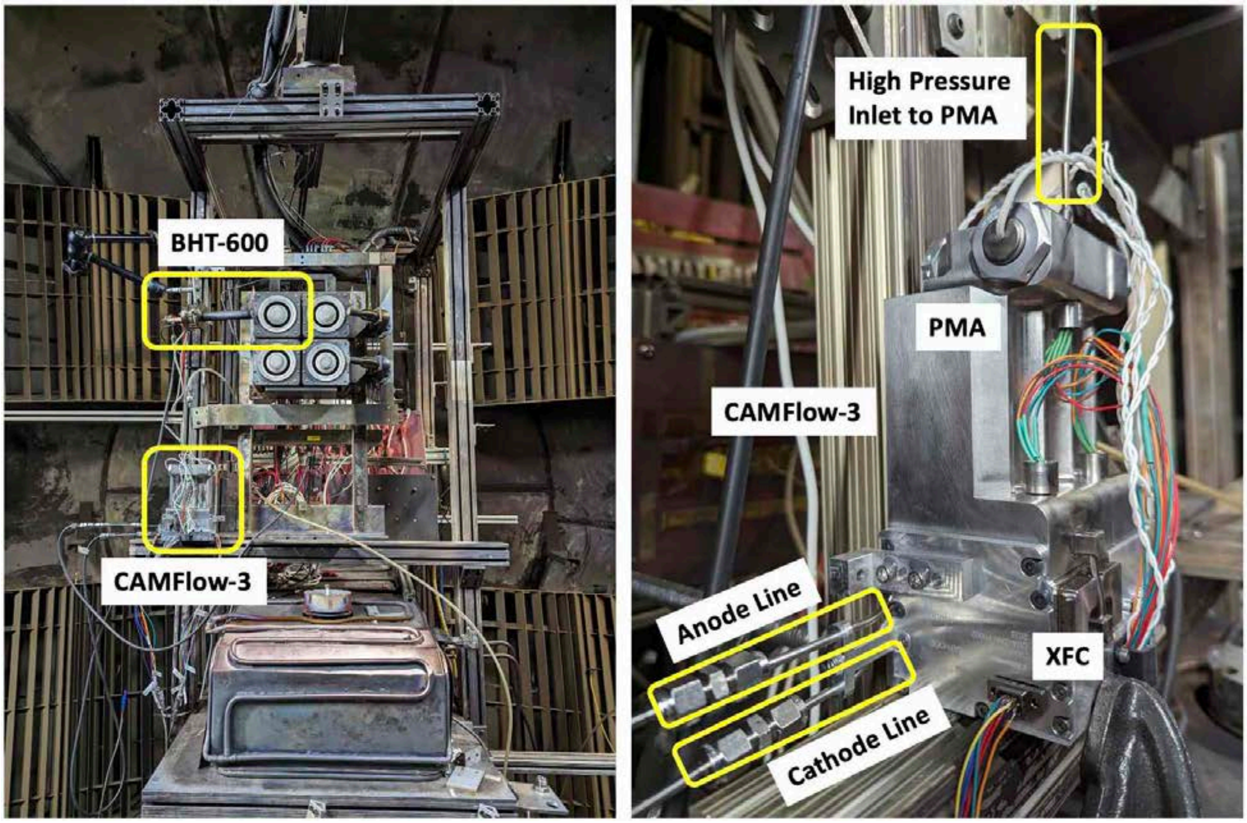

Figure 7. (Left) CUA CAMFlow-3 system integrated into the UM BHT-600 test rig. (Right) CAMFlow plumbed into UM system with gas lines into the PMA and out to the cathode and anode.

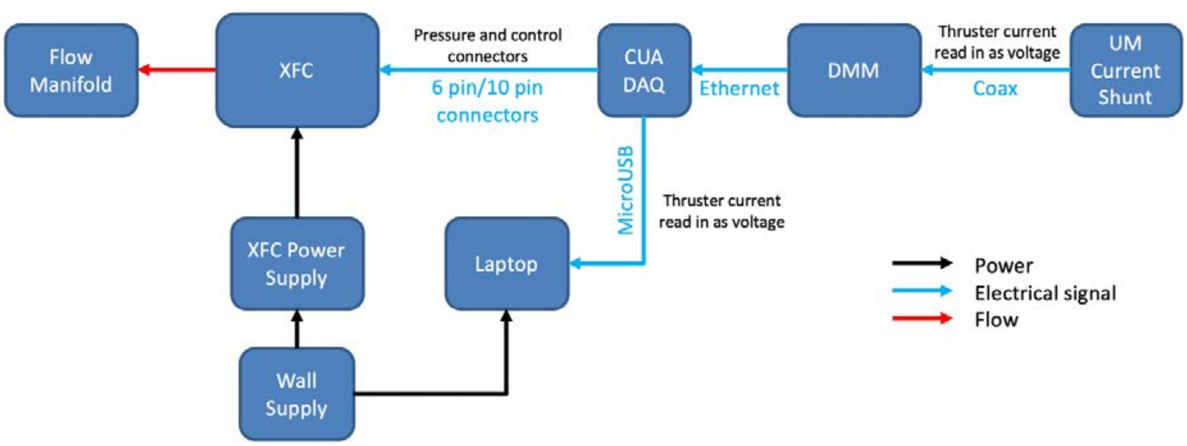

Figure 8. I/O configuration for the CUA CAMFlow controller (XFC) during the system integrated test.

Results of Thruster Testing with CAMFlow-3

The CUA XFC was delivered to UM and integrated with the laboratory flow system by UM personnel. It was shown that the XFC could operate in open-loop mode, serving the same function as a standard laboratory PMA and flow controller. UM was able to adjust the flow rate in a controlled way and in turn start the thruster and throttle the discharge current over the conditions shown in **Table 2**. During the learning phase of the pre-environmental test series, there was a fair amount of signal noise in all signals and is not shown for brevity. Some of this was cleaned up for the post-environmental series and the data is much easier to interpret and is discussed and shown below. **Figure 9** shows the BHT-600 operating when fed by the CAMFlow-3 system. The control currents and voltages tested from **Table 2** are illustrated in **Figure 10** for the pre-environmental test series.

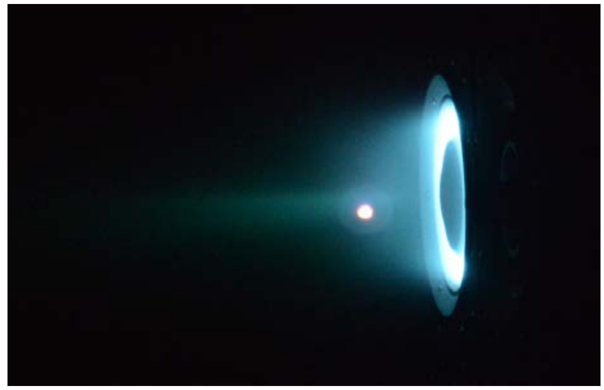

Figure 9: BHT-600 operating using CAMFlow-3 feed system at UM. The LaB6 cathode is observed as a small orange dot downstream of the thruster head.

CAMFlow capabilities were largely demonstrated operating in closed loop mode. In this case, UM commanded a set point for discharge current, and the controller employed a PID feedback loop to adjust flow to the thruster (which scales linear with discharge current) until this set point was achieved. **Figure 11** shows the closed loop test sequence that was run corresponding to the throttling points listed in **Table 2**. This depicts the set point as commanded to the thruster and the corresponding measured discharge current.

The set point was systematically adjusted over the test series to demonstrate the ability to throttle across all of the operating conditions shown in **Table 2**. In all cases, the thruster and controller operation both remained stable. After successful demonstration of controlled throttling, the thruster was shut down 0.5 hours into the run, and a hard start was performed in closed-loop mode. This objective was demonstrated by the controller responding successfully and stably, reducing the flow to achieve the nominal discharge current set point.

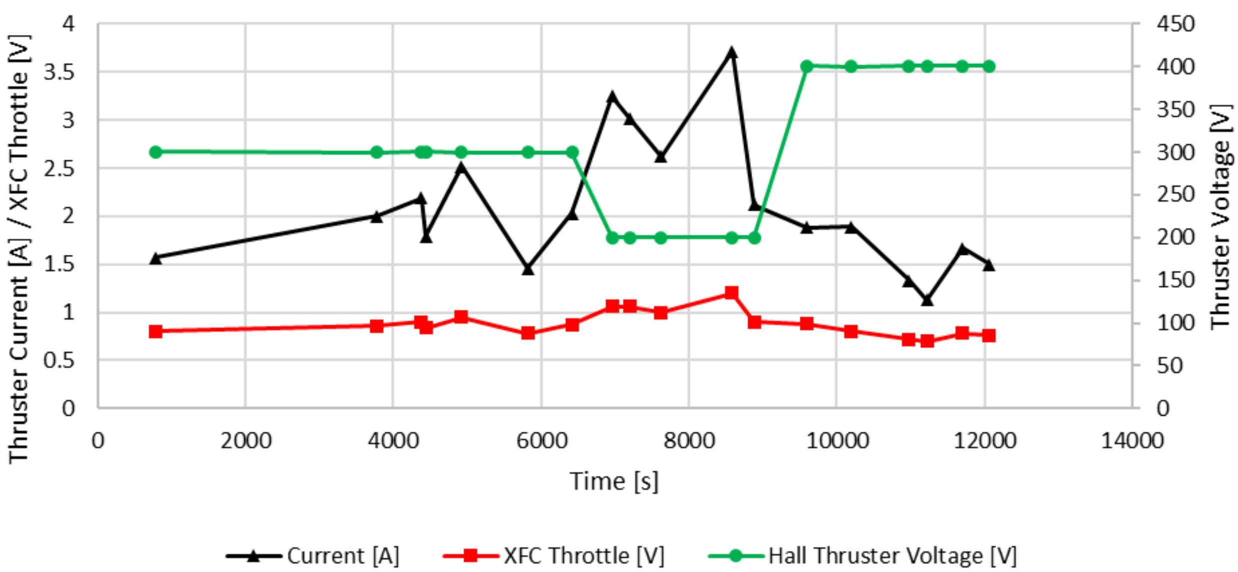

Figure 10. Throttle table test series in used in the pre-environmental testing. A similar series was used in the post-environmental testing, but at a faster pace (approximately 8300 seconds vs. 12000 seconds).

Figure 12 shows a close up of the transition between 400V-1.7A to 400V-1.5A. It also captures two of the PMA recharges. Note that the XFC control voltage rises slowly in between PMA valve actuations as the PMA pressure decreases and then the XFC voltage drops when the PMA valve actuates to raise the PMA pressure (showing up as a spike in the current read voltage). During all of this testing the controller was a little slow to soften the PMA recharges, but tuning of the system gains can smooth this out considerably. In other words, the drops in current with PMA recharge can be reduced with stronger gains and the spikes are in part a result of noise from the length of electrical lines to the DAQ system. In all cases the CAMFlow controller adjusts in a reasonably short time such that the current readback reaches and stabilized to the desired PID target current.

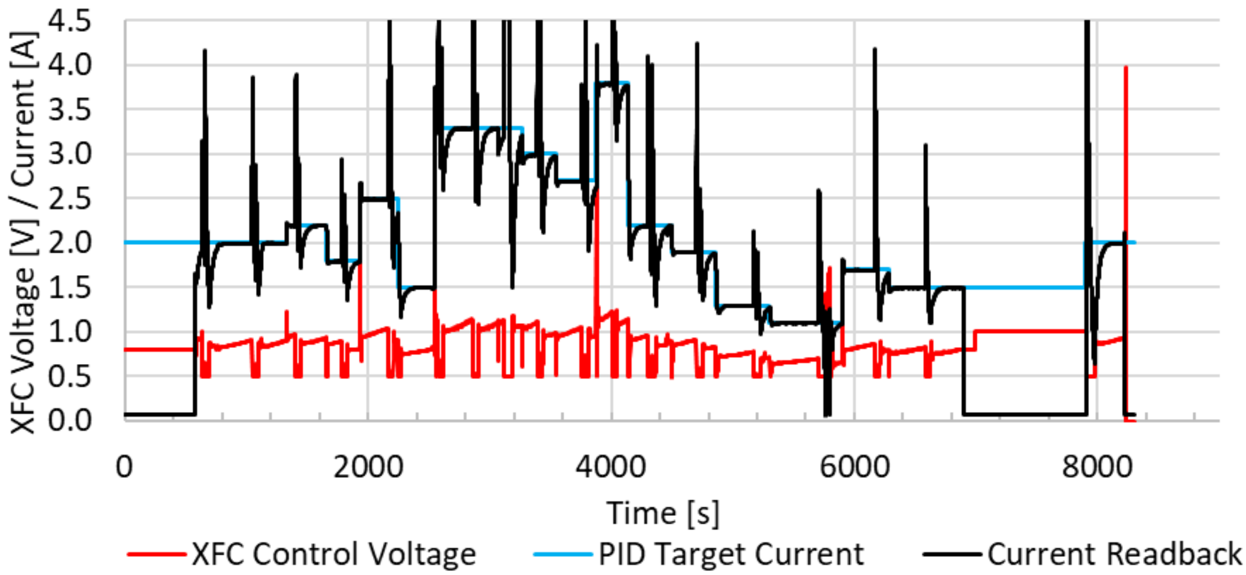

Figure 11. Complete throttle table test series in closed loop mode (post-environmental testing). The hard start case was performed at approximately 7800 s. Spikes in the signals occur when the PMA cycles resulting in noise from the length of the electrical lines to the DAQ system. The XFC control voltage rises slowly in between PMA valve actuations as the PMA pressure decreases.

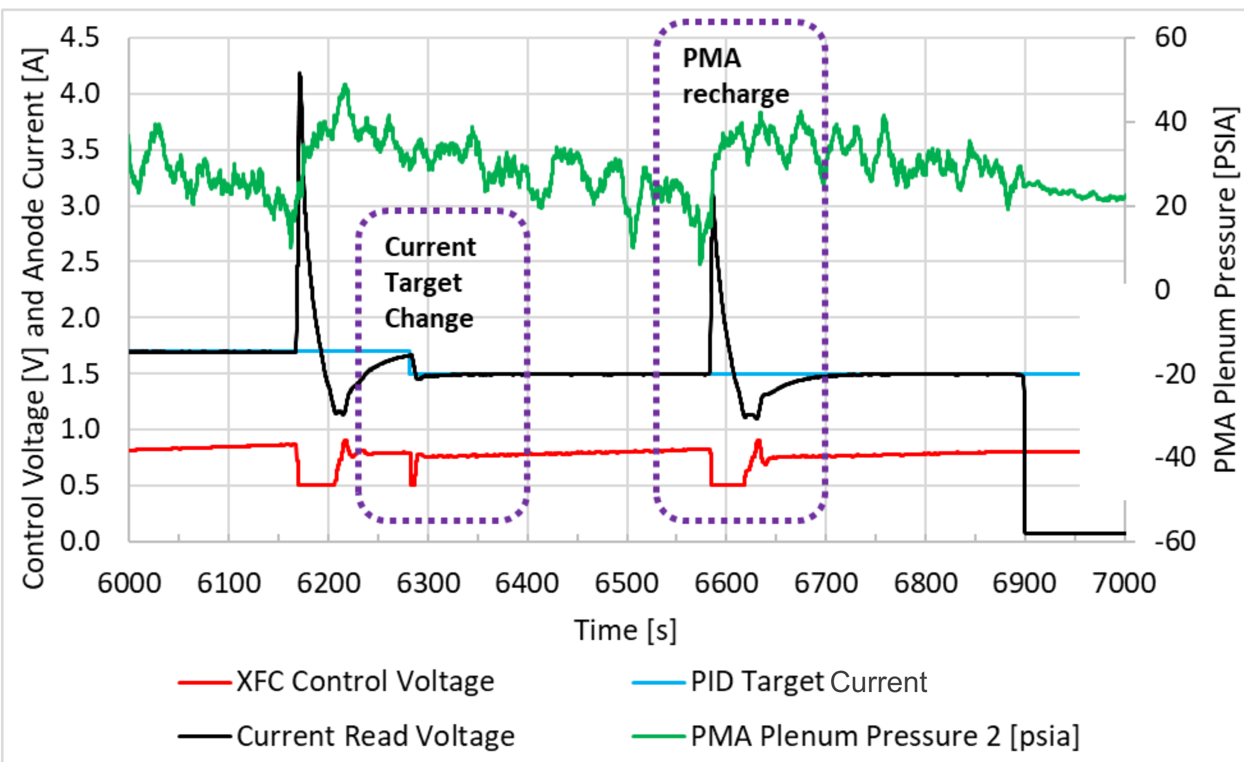

Figure 12. Telemetry from current transition testing (a close up from Figure 40). The commanded discharge current set point and the measured discharge current are shown. Note that there is noise in the pressure signal due to the length of the electrical lines to the DAQ system.

Figures 13 and 14 show source tank pressure and the two PMA pressures for pre-environmental and post-environmental testing, respectively. The source pressure was run at a lower value of ~140 psi to force the PMA valves to draw more power as a more stringent test of the system. The results are effectively the same and show that the system performed well pre- and post-environmental testing.

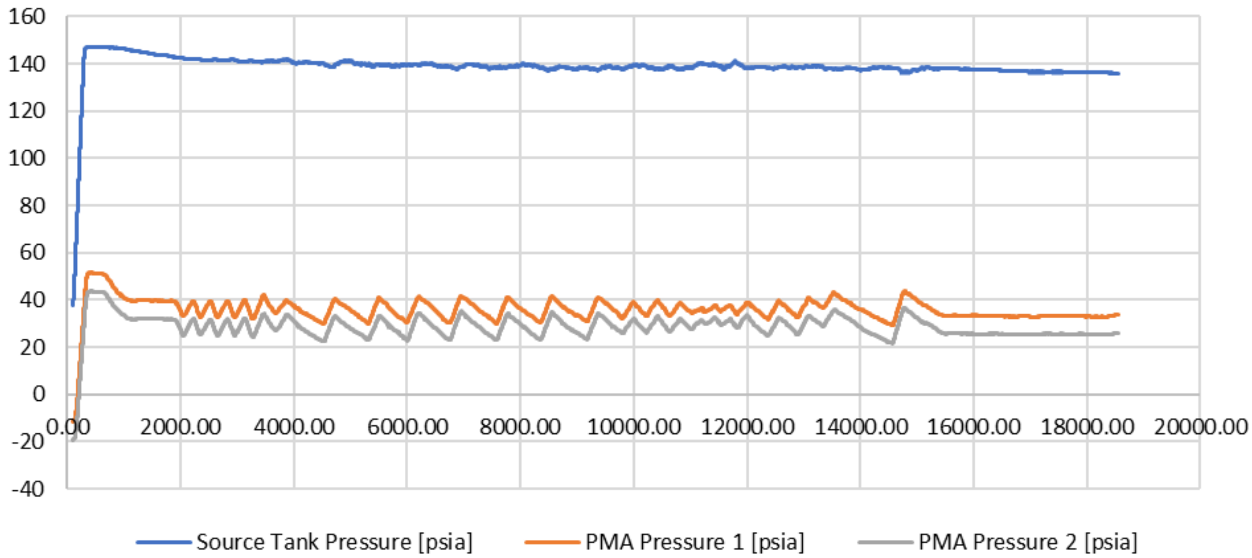

Figure 13. Source tank pressure and the two PMA pressures for pre-environmental testing. Note that one of the PMA pressure signals is lower due to differences in the length of the electrical lines to the DAQ system, but the behavior is the same (short electrical lines show the same value).

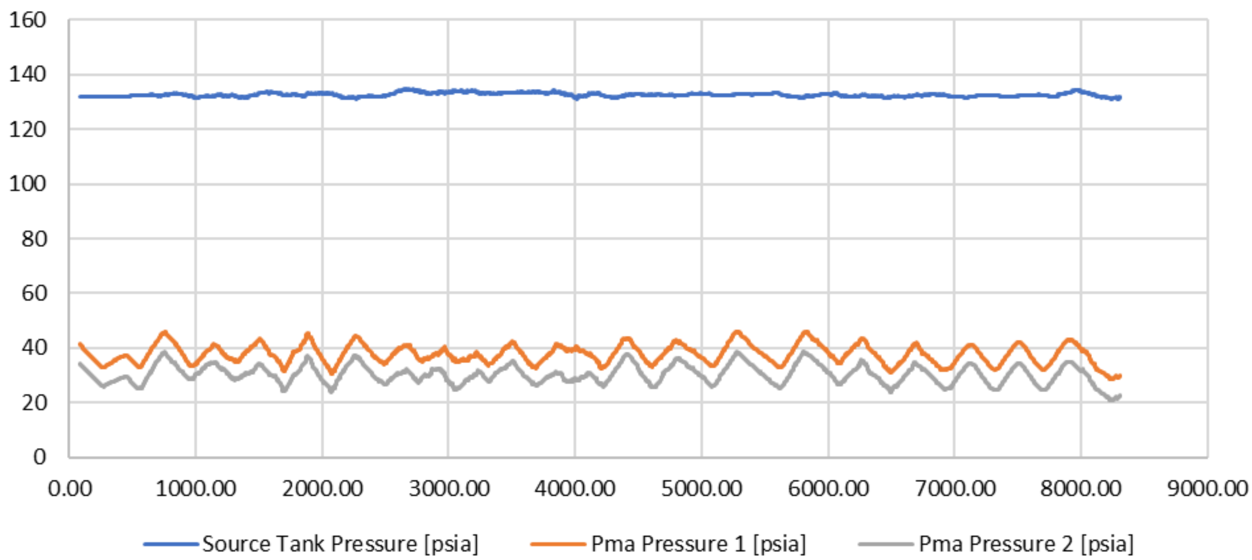

Figure 14. Source tank pressure and the two PMA pressures for post-environmental testing. Note that one of the PMA pressure signals is lower due to differences in the length of the electrical lines to the DAQ system, but the behavior is the same (short electrical lines show the same value).

<u>Testing Conclusions</u>

All the planned objectives for the systems level test were met during this Phase II activity. UM successfully demonstrated the ability of the CAMFlow-3 flow controller to integrate in a laboratory setting with a low power Hall thruster and to control its operation.

IV. Environmental Verification of CAMFlow-3 Hardware

3.1 Vibration Testing

The vibration table used at the University of Michigan Space Physics Research Laboratory (SPRL) environmental test facility is an Unholtz Dickie 560, **Figure 15**. This facility was also used by CUA on other NASA-funded programs. The requirements for vibration testing are specified by the qualification levels in NASA GEVS (GSFC-STD-7000b) for items 50 lbs or less (14.1 Grms).

For required environmental testing including random vibration and thermal vacuum cycling, the flight-like CAMFlow unit was mounted to an aluminum plate. In the case of vibration testing, this plate will be mounted to the face of the vibration table. The plate has been specially designed for vibration testing purposes and has been designed with appropriate mass and dimensional characteristics to not influence the results of the test. For TVAC, the plate will be cooled and warmed as necessary to assist in the thermal cycling of the unit via conduction, and this was modified with an additional hole pattern to accommodate the CAMFlow system, **Figure 16**.

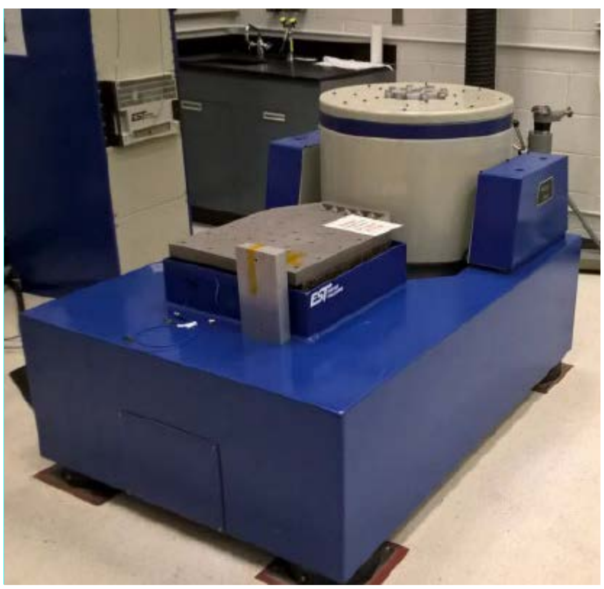

Figure 15. SPRL Unholtz-Dickie UD-206H vibration table.

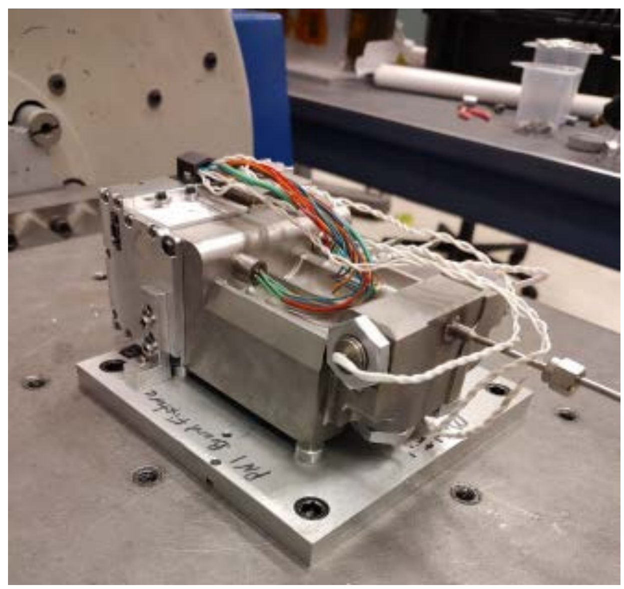

Figure 16. CAMFlow-3 unit mounted to the test plate. The distal holes are used for mounting to the vibe table, and (unseen) the proximal holes are used to mount the unit to the plate.

A sequence of vibrations tests were completed in each of the orthogonal axis. In each axis there was a low-level sine sweep (20-2000 Hz; 0.25 g; 4 Octaves/min) prior to and after a qualification level random vibration test (14.1 Grms GEVS). The low-level sine sweeps were used to evaluate any change in the structure. An accelerometer was glued to Kapton tape added to the body to evaluate response of the structure.

Figure 17 shows the random level of excitation during the X-axis testing. **Figure 18** shows the sine response in the X-direction of the response. A shift of 16% is larger than normal, but as determined after the X & Y testing, a #8 screw was missing, and a spacer could rotate which indicate a change in the mounting stiffness as shown in **Figure 19**. No other structural changes could be observed apart from that. Change in stiffness at that mounting point could easily account for frequency shift.

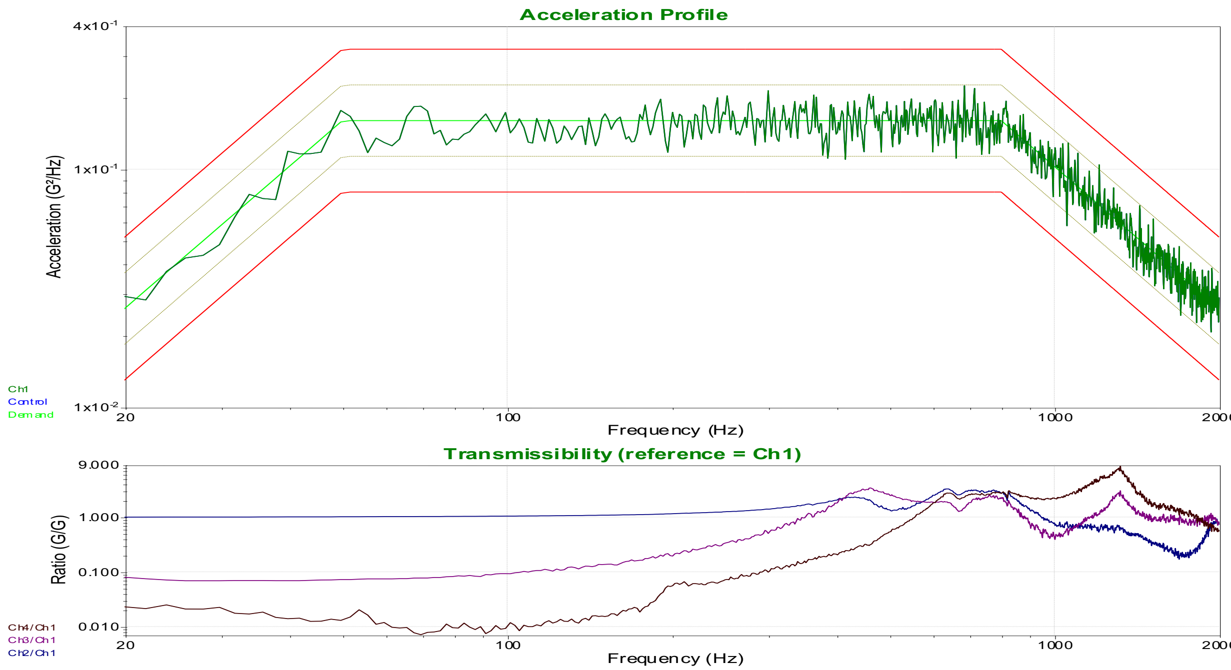

Figure 17. X Axis random vibration.

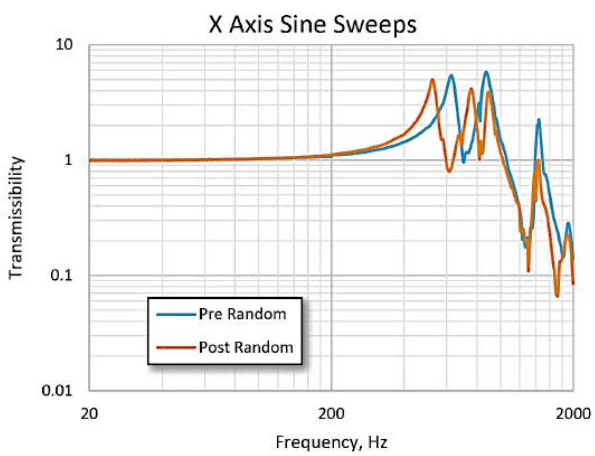

Figure 18. X axis sine sweeps before and after random vibe. First mode 627 Hz -> 525 Hz (16% shift).

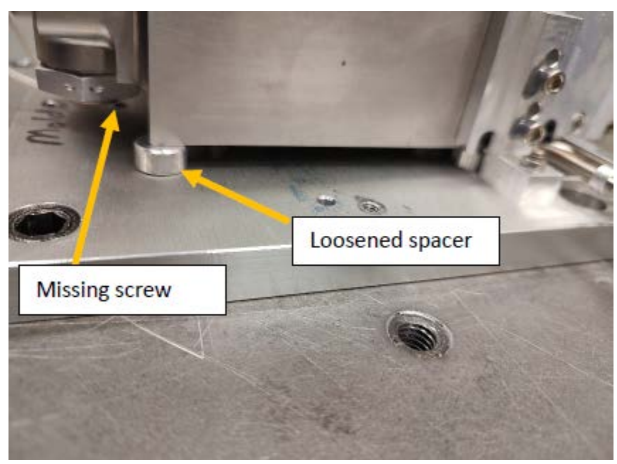

Figure 19. View of loose stand off and location of missing screw in X&Y testing.

The sine sweeps in the Y-axis were similar in character (not shown for brevity) and also indicated a similar shift of 16% as with the X-axis testing. The fact that it is the same percentage shift as the X-axis appears coincidental. The shift is expected to be from the same reason as the X-axis and not indicative of a structural failure. For the Z-axis testing, when reconfiguring the test article on the interface plate, the absence of the #8 screw was noted and added. The natural frequency was much higher (first mode 1559 Hz, not shown for brevity) than in the X & Y–axis testing and a negligible shift (~1%) was measured. Both of these latter observations were likely due to the additional screw added to support CAMFlow. The vibration qualification testing completed successfully with no discernable structural change and functionality confirmed prior to and after testing.

3.2 Thermal Vacuum Testing

The facility to be used for the TVAC testing is the "blue" TVAC chamber at the University of Michigan's SPRL, **Figure 20**. This chamber has an internal volume 36" in diameter and 48" long. It is capable of -55 to 150°C and a base pressure < $5x10^{-6}$ torr.

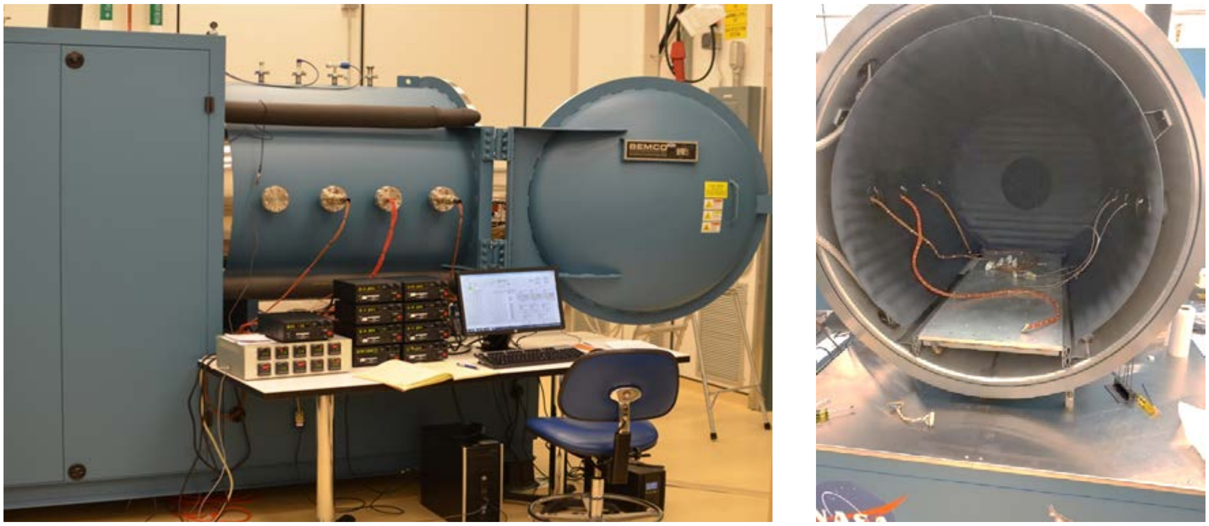

Figure 20. SPRL "blue" TVAC chamber. CAMFlow-3 mounted inside in right photograph.

CAMFlow was connected to an interface plate via #6 screws and a thermal gasket was used under the two feet to aid in heat transfer to the body. **Figure 21 (left and right)** shows the isometric and top view of CAMFlow in the test setup for TVAC. The wire harness is shown along with the two thermocouples used to measure the interface plate temperature. It was these temperatures that were used to establish the dwell requirements.

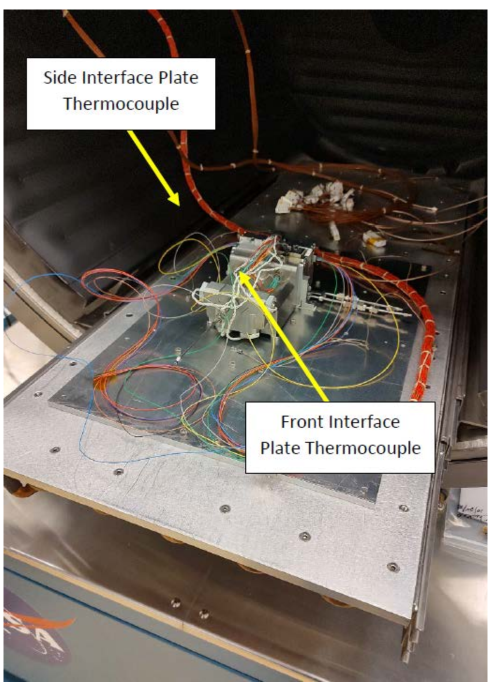

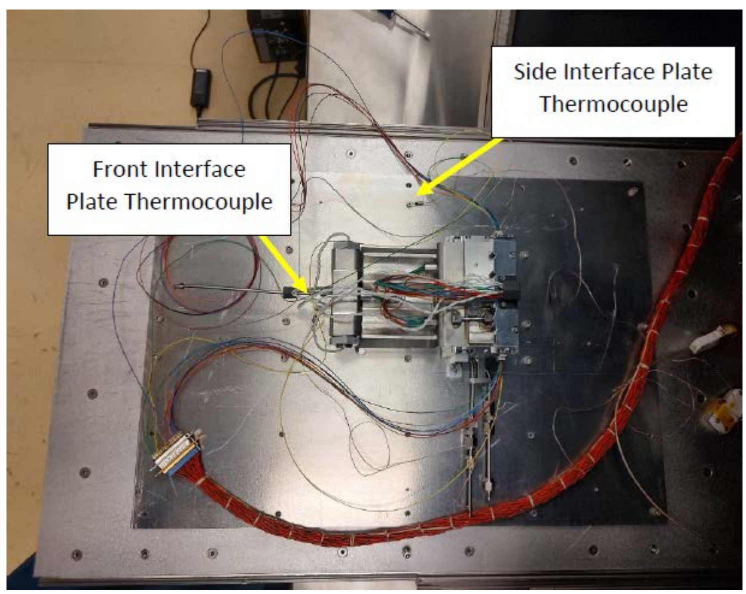

Figure 21. Left: Isometric view of the platen with installed CAMFlow unit. Right: Top view of the platen with installed CAMFlow unit.

The test successfully achieved 4 hot and cold dwells of at least 1 hour at temperatures of 60 +/-2 ºC and -20 +/-2 ºC. The rate of change between dwells was <5 ºC/min and was typically around 4 ºC/min. **Figure 22** shows the temperatures recorded for the interface plate throughout the duration of the test. The power supplies provided the necessary power to CAMFlow through pins 29, 31, 33, 35, and 37 throughout the duration of the test. The power was initiated prior to the temperature cycling, was turned off after the hot third cycle while the test was paused for the night and started up again prior to continuing to the third cold cycle and then turned off after the final functional test following the completion of the temperature cycles.

Figure 23 contains the currents displayed on the power supplies through the test. The currents when En1, En2, XFC Chain, and XFC Control were grounded indicate the baseline condition that was maintained throughout the duration of the test. Minimal variation (≤0.02 A) of the results occurred throughout the duration of the test for the baseline values. Values above 0.02 A were a result of the functional tests. The results of the functional tests are also given in **Table 3**.

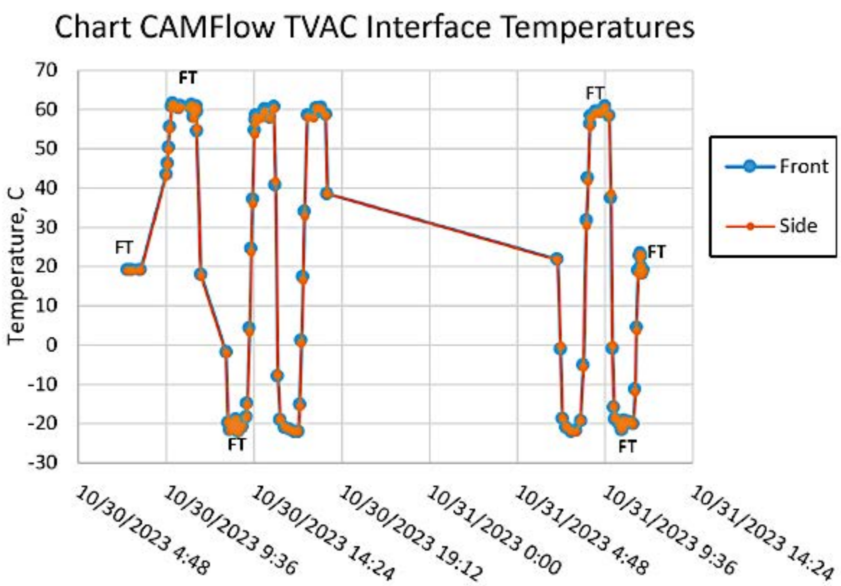

Figure 22. Platen temperatures during thermal vacuum testing. Dwell temperatures +60 to -20 °C (+/-2 °C) for a minimum of 1 hour. FT corresponds to functional testing occurred.

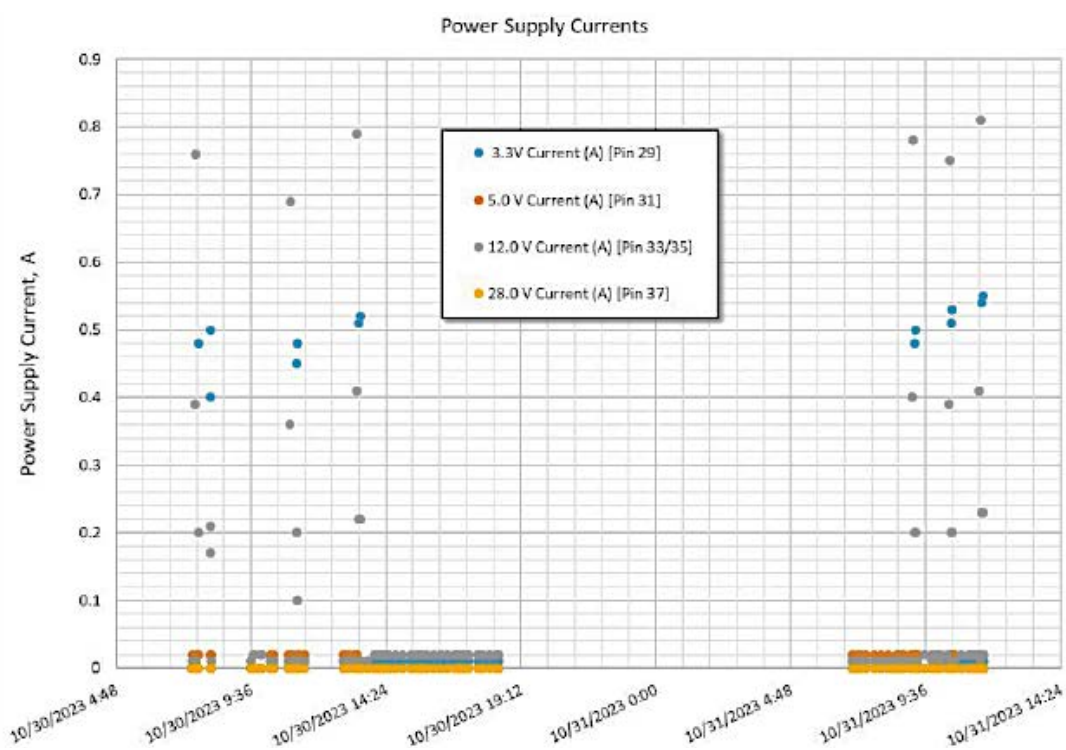

Figure 23. Power supply currents displayed during TVAC testing.

Table 3. TVAC functional test results.

			Power Supply Currents, A				Voltage on Pin, V			
Cycle	Temp	Pressure, x10^{-6} Torr	3.3V	5.0 V	12.0 V	28.0 V	En1	En2	XFC Chain	XFC Control
BOT	19	22.5	0.00	0.02	0.01	0.00	0	0	0	0
BOT	19	7.5	0.01	0.00	0.39	0.00	3.3	0	0	0
BOT	19	9.2	0.00	0.00	0.76	0.00	3.3	3.3	0	0
BOT	19	840	0.48*	0.02	0.20*	0.00	0	0	0	3.3
BOT	19	99	0.40*	0.02	0.17*	0.00	0	0	0	3.3
BOT	19	110	0.50*	0.02	0.21*	0.00	0	0	3.3	3.3
1	61	11	0.00	0.02	0.01	0.00	0	0	0	0
1	61	12	0.02	0.00	0.36	0.00	3.3	0	0	0
1	60	10	0.00	0.00	0.69	0.00	3.3	3.3	0	0
1	60	57	0.45*	0.02	0.20*	0.00	0	0	0	3.3
1	61	100	0.48*	0.02	0.10*	0.00	0	0	3.3	3.3
1	-21	0.2	0.02	0.01	0.02	0.01	0	0	0	0
1	-20	1.0	0.02	0.02	0.41	0.00	3.3	0	0	0
1	-20	1.1	0.00	0.00	0.79	0.00	3.3	3.3	0	0
1	-20	430	0.51*	0.02	0.22*	0.00	0	0	0	3.3
1	-22	52	0.52*	0.02	0.22*	0.00	0	0	3.3	3.3
4	59	3.8	0.00	0.02	0.01	0.00	0	0	0	0
4	59	4.3	0.01	0.00	0.40	0.00	3.3	0	0	0
4	59	4.5	0.00	0.00	0.78	0.00	3.3	3.3	0	0
4	59	49	0.48*	0.02	0.20*	0.00	0	0	0	3.3
4	59	17	0.50*	0.00	0.20*	0.00	0	0	3.3	3.3
4	-20	0.2	0.02	0.01	0.00	0.02	0	0	0	0
4	-20	0.7	0.02	0.00	0.39	0.00	3.3	0	0	0
4	-20	0.9	0.00	0.00	0.75	0.00	3.3	3.3	0	0
4	-20	24	0.51*	0.00	0.20*	0.00	0	0	0	3.3
4	-22	33	0.53*	0.00	0.20*	0.00	0	0	3.3	3.3
EOT	22	0.3	0.01	0.00	0.02	0.00	0	0	0	0
EOT	23	0.7	0.02	0.00	0.41	0.00	3.3	0	0	0
EOT	23	0.9	0.00	0.00	0.81	0.00	3.3	3.3	0	0
EOT	18	19	0.54*	0.00	0.23*	0.00	0	0	0	3.3
EOT	18	31	0.55*	0.00	0.23*	0.00	0	0	3.3	3.3

*Currents pulsed between zero and rapidly to value indicated

3.3 Performance Verification w/ Thruster

This testing consisted largely of a repeat of critical performance tests conducted in **Section III** to verify the CAMFlow-3 system was still operating nominally post-environmental testing (vibe and TVAC). **Table 4** lists the 15 different thruster operating parameter sets (magnet current, voltage, and target current) for the pre- and post-environmental testing and the differences. Note that the actual XFC control voltage gradually increases during PMA blowdown between PMA valve cycles, therefore all values listed are approximately the median value used by the XFC to attain the target thruster current. During pre-environmental testing this was manually controlled. For post-environmental testing the current readback was incorporated and the throttle table was followed using closed loop control. The XFC control voltages are in good agreement before and after testing, to within an average of < 2% error, which is within the original goal of < 3% flow variation. See **Section III** for additional post-environmental test data. In summary, CAMFlow-3 underwent vibrational and thermal vacuum testing; its performance was effectively the same before and after the environmental testing.

Table 4. Pre- and post-environmental test results for current and control voltage.

Thruster Parameters			Pre-environmental Testing		Post-environmental Testing		Difference	
Magnet Current (A)	Voltage (V)	Target Current (A)	Actual Current (A)	XFC Control Voltage (V)	Actual Current (A)	XFC Control Voltage (V)	Actual Current (%)	XFC Control Voltage (%)
2	200	2.2	2.06	0.9	2.19	0.94	6.3	4.4
2	200	2.7	2.62	1	2.67	1.02	1.9	2.0
2	200	3	3.02	1.06	2.99	1.09	–1.0	2.8
2	200	3.3	3.25	1.06	3.28	1.1	0.9	3.8
2	200	3.8	3.7	1.2	3.78	1.17	2.2	–2.5
2	300	1.5	1.47	0.78	1.5	0.78	2.0	0
2	300	1.8	1.79	0.84	1.79	0.8	–5.0	–4.8
2	300	2	2.03	0.87	1.99	0.89	2.3	2.3
2	300	2.2	2.19	0.9	2.17	0.9	–0.9	0
2	300	2.5	2.46	0.95	2.49	1.01	1.2	6.3
1.5	400	1.1	1.11	0.7	1.1	0.68	–0.9	–2.9
1.5	400	1.3	1.3	0.72	1.3	0.76	0	5.6
1.5	400	1.5	1.5	0.76	1.49	0.79	–0.7	3.9
1.5	400	1.7	1.67	0.78	1.7	0.83	0	6.4
1.5	400	1.9	1.88	0.88	1.89	0.89	–0.5	1.1
						AVERAGE %:	0.5	1.9

V. Thermal Modeling

Thermal Model Description

The primary objective of the thermal modeling for CAMFlow was to determine an expected thermal range of the system. The design of CAMFlow-3 from **Section II** was taken and a thermal model was developed for the system with 3 space-rated pressure sensors (the large cylinders in **Figure 24**) and 2 XFCs. The updated geometry of CAMFlow was modeled in Thermal Desktop with 1597 nodes. The model in Thermal Desktop is built from primitive shapes that are part of Thermal Desktop's library. Images in **Figure 24** show the overall model. Simulations were performed for both "Nominal Operating Conditions" and the "Hot Operating Mode" when mounted inside a spacecraft, external to a spacecraft, and when enclosed in a simple aluminum box to provide some minimal thermal shielding. Extra attention is paid following the thermal path from the circuit boards to the structural supports since the bulk of the power dissipated is on the circuit boards. **Table 5** lists the heats applied and location in the model.

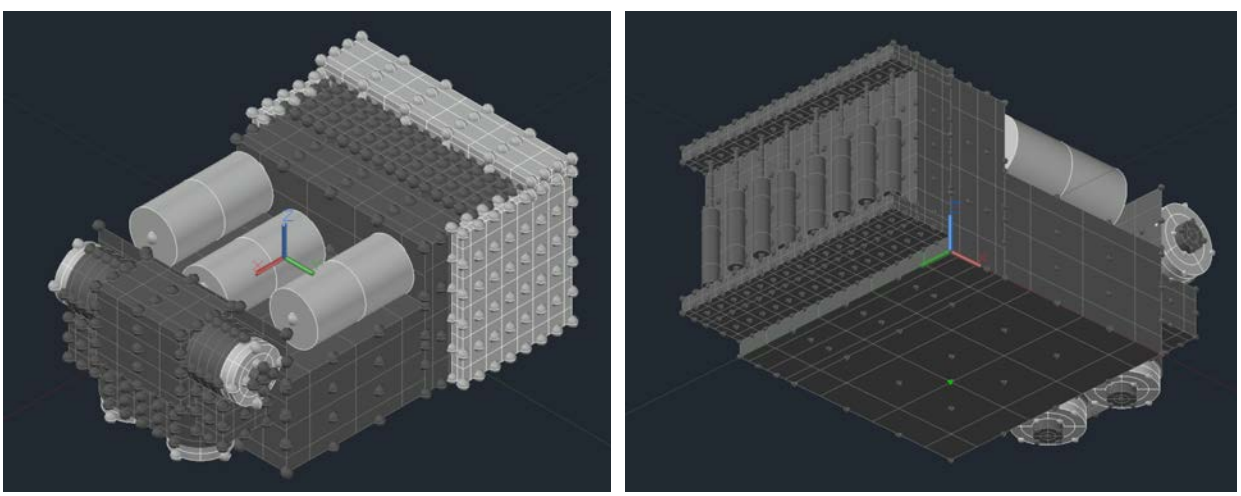

Figure 24. Screen captures of flight-like prototype CAMFlow system as modeled in Thermal Desktop with 1597 nodes. (Left) model from one perspective showing aluminum plates on left that enclose the XFC and circuit board, and (right) perspective from the other side with enclosure plates removed.

Table 5: List of heats applied for each primary location in the modeled CAMFlow system.

Location	Hot Case (EOL - cold cathode start)	Cold Case (Idle)	Mid Life Nominal
Pressure Sensors	0.06	0.06	0.06
PMA Valve Chain 1 (PMA1)	4.8	0	0.08
PMA Valve Chain 2 (PMA2)	4.8	0	0
XFC Valve Chain 1 (XFC1)	1.68	0	0.84
XFC Valve Chain 2 (XFC2)	0	0	0
XFC Cathode Valve Chain 1 (XFCC1)	1.68	0	0
XFC Cathode Valve Chain 2 (XFCC2)	0	0	0
Heat Generated by PCB	1.043	0.268	0.36
Total	**14.06**	**0.328**	**1.34**

Thermal simulations were refined to best represent the hardware. Part of this refinement was the adjustment of interfaces within the structures to capture a reasonable approximation of this thermal conductivity. This model includes values of the emissivity and absorptivity of the surfaces that will enable evaluation of radiation heat transfer with the environment or hot structures such as a hall thruster. The model was also refined to best locate the internal heating within the structure. Note that two XFCs and one PMA are modeled here as the dual XFC unit will have higher power draw and heating than a single XFC system, i.e., the dual XFC system will provide a more extreme case.

Assumptions made in the thermal modeling include:

- Boundary Conditions
  - Mounted to a spacecraft through bolts. Spacecraft is at 300 K.
  - Instrument is exposed and radiating to space.
    - Aluminum is alodined (ε=0.1, α= 0.45)
    - Stainless steel is bare (ε=0.14, α= 0.47)
- Stainless steel parts are all welded
- PMA valves held in place by pressure from the nut
- XFC valves are clamped with indium foil
- Thermal Conductivity
  - Aluminum: 167.9 W/mK
  - Stainless: 16.3 W/mK (order of magnitude lower than aluminum)
- Dissipations averaged over surfaces
  - i.e., PCB dissipation on entire board
- Uncorrelated model (no test data)
  - Uncertainty around 10-15ºC

Simulations of Flight-like Prototype CAMFlow: Normal Operating Mode

Under nominal operation most components are within 20°C of the spacecraft mounting temperature (27°C), **Figure 25**. When the controller is mounted outside of the spacecraft with a view of space it tended to operate below the interface temperature from 7 – 30°C. When inside the spacecraft it operated warmer without the cold view to space; this range was from 27 – 40°C. Assumed heating for the circuit board and valves for nominal conditions are:

Circuit Board = 0.36 W
PMA Valve1 = 0.08 W PMA Valve2 = 0.00 W
XFC Valve1 = 0.84 W XFC Valve2 = 0.00 W

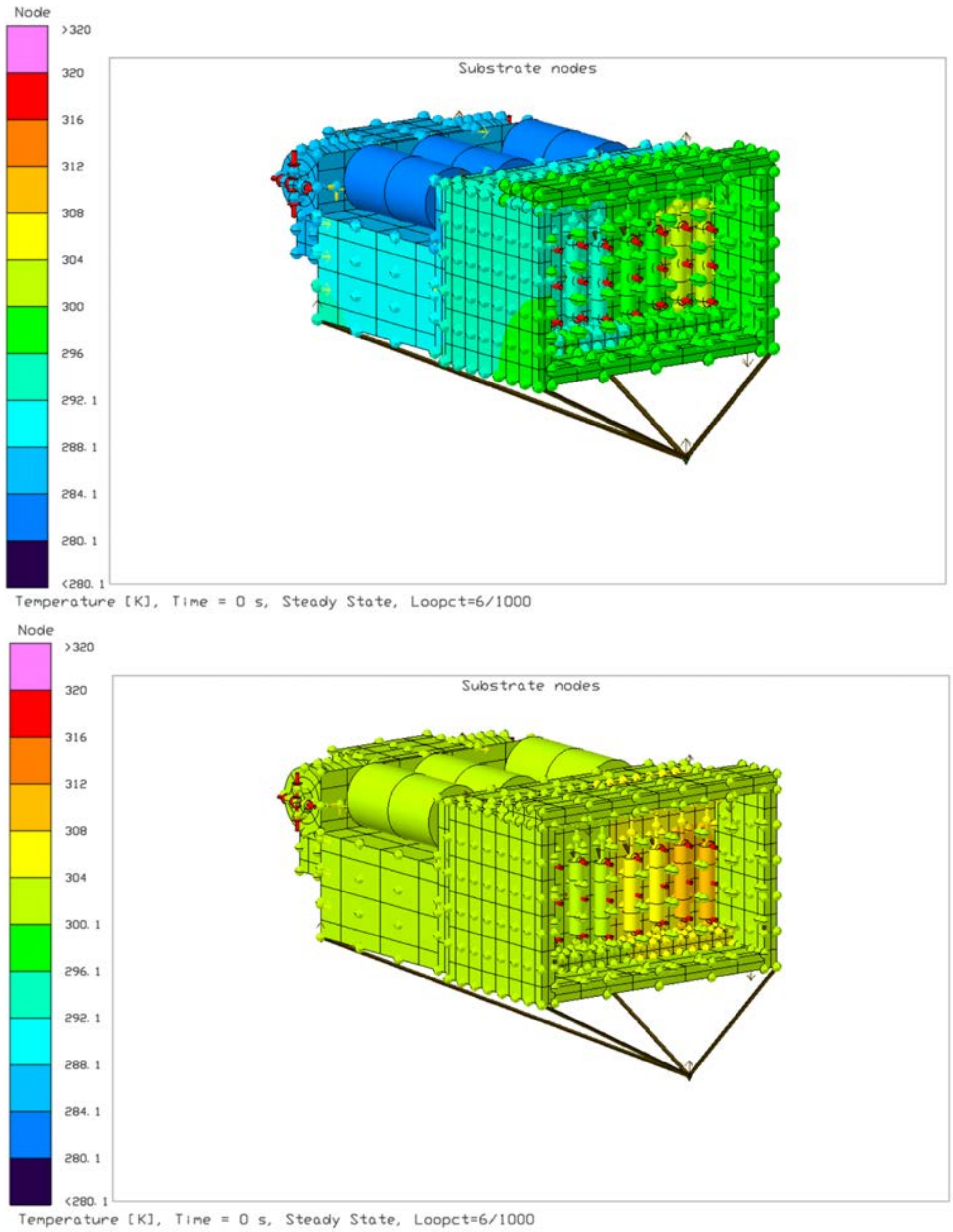

Nominal Conditions: CAMFlow mounted <u>external</u> to spacecraft w/ open view of space

Nominal Conditions: CAMFlow mounted <u>inside</u> spacecraft w/o cold view of space

Figure 25. Screen captures of flight-like prototype CAMFlow system as modeled in Thermal Desktop with 1597 nodes under "nominal" operating conditions. (Top) cooler operation when mounted <u>external</u> to spacecraft with open view of space, and (bottom) warmer operation when mounted <u>inside</u> spacecraft without cold view of space.

<u>*Simulations of Flight-like Prototype CAMFlow: Hot Operating Mode (External and Internal)*</u>

Under extreme "hot" operating conditions the components naturally are much warmer than the nominal operation, **Figure 26**. When the controller is mounted outside of the spacecraft with a view of space it tended to operate from 30 – 65°C. When inside the spacecraft it operated warmer without the cold view to space; this range was from 30 – 85°C. Assumed heating for the circuit board and valves for hot operating conditions are:

Circuit Board = 1.04 W
PMA Valve1 = 4.80 W PMA Valve2 = 4.80 W
XFC Valve1 = 1.68 W XFC Valve2 = 1.68 W

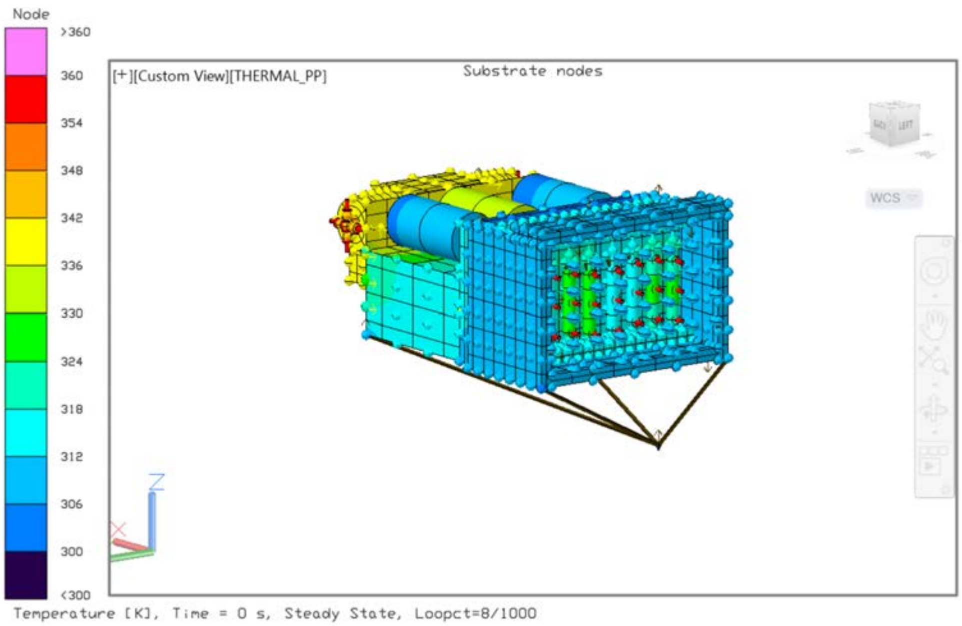

Hot Case Conditions: CAMFlow mounted <u>external</u> to spacecraft w/ open view of space

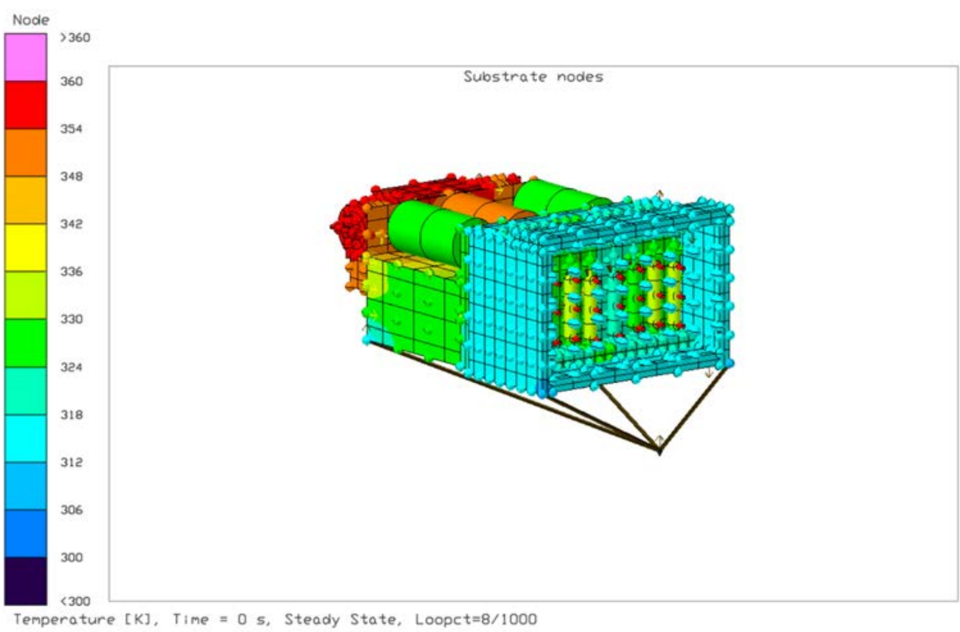

Hot Case Conditions: CAMFlow mounted <u>inside</u> spacecraft w/o cold view of space

Figure 26. Screen captures of flight-like prototype CAMFlow system as modeled in Thermal Desktop with 1597 nodes under "hot case" operating conditions. (Top) cooler operation when mounted <u>external</u> to spacecraft with open view of space, and (bottom) warmer operation when mounted <u>inside</u> spacecraft without cold view of space.

<u>Simulations of Flight-like Prototype CAMFlow: Hot Operating Mode (Inside Aluminum Box)</u>

The final thermal simulations were performed for the high-power case ("Hot Operating Mode") where CAMFlow was enclosed in a simple aluminum box (emissivity =0.1). This box was not conductively tied to anything and simply in the path of radiant heat transfer with space. It would effectively be like having a single layer of MLI around an exterior mounted unit. The spacecraft mount is at 27°C. Unit temperatures that result range from 30 – 76°C, **Figure 27**. Temperatures are warmer than the external (**Figure 26-top**) CAMFlow by about 10°C, but cooler than being mounted inside (**Figure 26-bottom**) the spacecraft by 10°C. As additional layers of MLI are added the temperatures will be similar to the previously reported version mounted inside the spacecraft. Assumed heating for the circuit board and valves for hot operating conditions were the same as those given above.

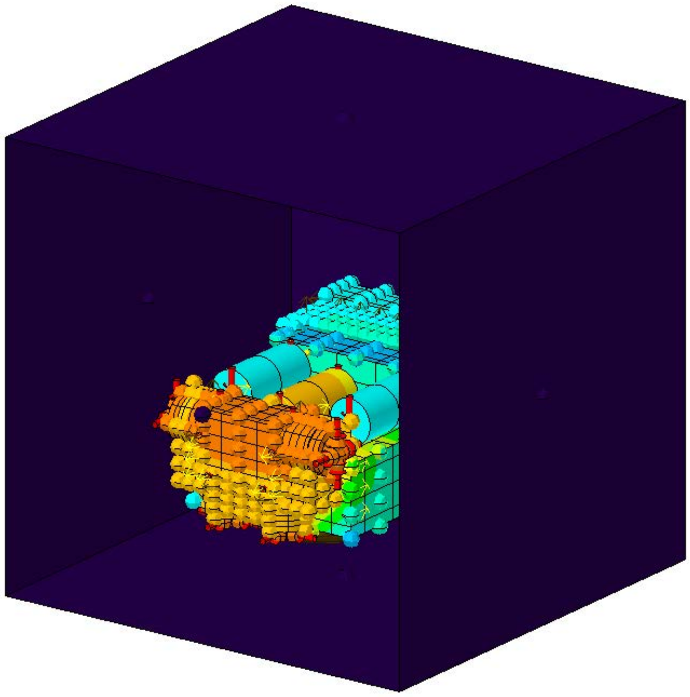

Hot Case Conditions: CAMFlow illustrated as being placed inside an aluminum box

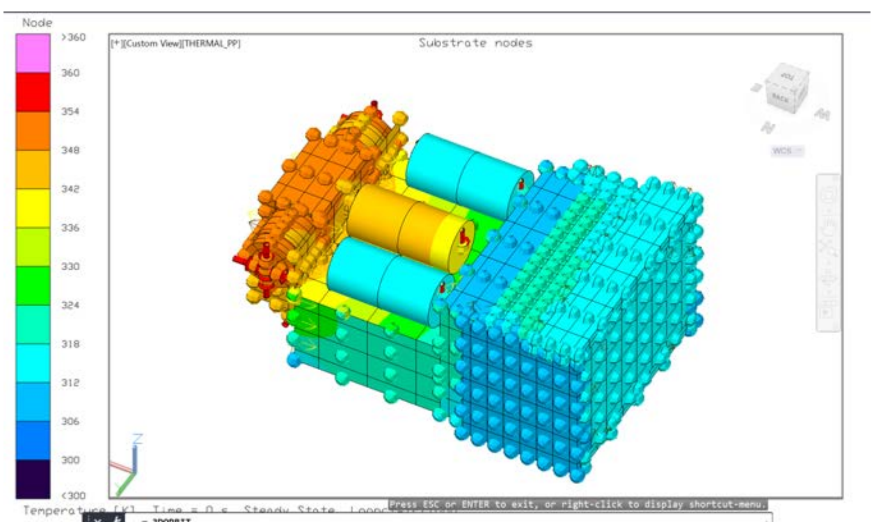

Hot Case Conditions: CAMFlow mounted inside an aluminum box

Figure 27. Screen captures of flight-like prototype CAMFlow system as modeled in Thermal Desktop with 1597 nodes under "hot case" operating conditions inside an aluminum box. (Top) illustrated inside the box, and (bottom) simulation results for temperature while operating in steady state.

Model Validation

During extended operation of CAMFLOW during hall thruster testing (**Figure 11**), an internal temperature measurement was recorded. The sensor was located on the power electronics board, which is in close thermal contact with the XFC valves. The test was run in a state most like the "Nominal Operating Conditions" of the thermal analysis, with single sets of valves in operation. **Figure 28.** below shows the temperature over the ~3 hours test duration.

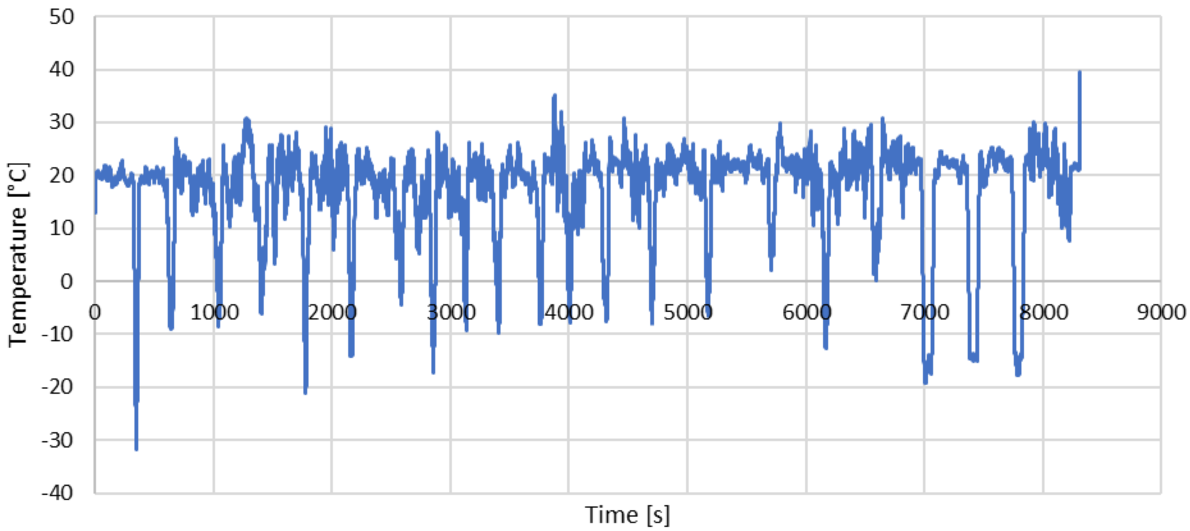

Figure 28. Internal temperature over time for nominal operating conditions.

While the CAMFLOW had some additional conductive cooling capability in a terrestrial vacuum tank, it was not hard mounted, and had low contact with the test fixture. The temperature measurement experienced significant noise, largely from the 10+ meters of cables carrying the analog reading. Further, voltage drops in the power carrying lines were significant enough to alter the temperature response. Despite this, the temperatures were corrected based on the amplifier circuit properties and initial temperature and rose < 5° C during the test. This is reasonably consistent with the minimal temperature rises seen in the XFC region of the thermal modeling (**Figure 25**).

VI. Concluding Remarks

CUA's compact CAMFlow-3 system is a highly reliable, fixed-frequency flow controller for electric propulsion systems and has now been tested to TRL 6. CAMFlow uses an innovative control scheme that enables stable operation, even for the low flow rates necessary for sub-kW Hall effect thrusters. This methodology reduces system complexity, places the onus of reliability on valve cycle life, and allows for a direct correlation between system life and valve cycle life. The stainless steel CAMFlow-3 unit has a mass of 2.78 kg and a volume envelope of 1,530 cm^3 (note that the mass could be reduced to ~1.9 kg if titanium was utilized instead of stainless). Additionally, during this work, two Lee Co. IEP control valves were cycled >100 million pulses (the equivalent of 300 kg Xe) while maintaining a very low leak rate of < 1e-4 scc/s helium.

The CAMFlow control scheme was successfully tested and validated on a 600-Watt Hall thruster at UM. This included open loop, closed loop, and cold cathode "hard" start operations. All the planned objectives for the CAMFlow-3 systems level test were met during this effort. UM successfully demonstrated the ability of the developed flow controller to integrate in a laboratory setting with a low power Hall thruster and to control its operation. CAMFlow-3 also underwent vibrational and thermal vacuum testing; its performance was the same before and after the environmental testing taking the system to TRL 6. Thermal modeling was supported by nominal operating test results.

While CAMFlow units are presently focused on smaller Hall-effect or gridded-ion electric propulsion systems having a flow rate in the 0 – 15 mg/s range, the technology is scalable and can be adapted for a large range of flow rates applicable to a broader commercial market. The packaging of the CAMFlow system elements is flexible and ultimately it will be the customers who will drive the preferred electronics placement and packaging.

A specific goal stated in NASA's 2015 Roadmap In-Space Propulsion Technologies Technical Areas 2.2.1, Electric Propulsion is "miniaturization of some of the electric propulsion concepts for emerging mission applications, such as CubeSat primary propulsion, highly accurate formation flying, and precision pointing for observatories has introduced some manufacturing challenges not previously experienced." CUA's use of Lee Co. microvalves and corresponding CAMFlow control system respond directly to this goal with a focus on miniaturized well-regulated performance with cost reduction through common COTS materials of construction. Aside from the general application of gas-fed propulsion systems, CAMFlow can also enable some unique ground testing opportunities. With open and closed loop control, along with the potential to use process variables aside from pressure, CAMFlow can help aid in the development of alternative control schemes a wide variety of fluid flow systems.

VII. Acknowledgments

This work was supported by NASA's STTR program on contract number 80NSSC21C0605 (technical monitor Timothy Grey) and by CUA Internal Research and Development funds.

VIII. References

Cardin, J., Cook, W., and Bhandari, R., "Qualification of an Advanced Electric Propulsion Xenon Flow Control Module," *33rd International Electric Propulsion Conference*, Washington, DC IEPC-2013-382, 2013.

Conversano, R., Goebel, D., Hofer, R., Mikellides, I., Wirz, R., "Performance Analysis of a Low-Power Magnetically Shielded Hall Thruster: Experiments," *Journal of Propulsion and Power*, Vol. 33, No. 4, pp. 975-983, 2017a.

Conversano, R., Goebel, D., Hofer, R., Arora, N., "Performance Enhancement of a Long-Life, Low-Power Hall Thruster for Deep Space Smallsats," *IEEE Aerospace Conference*, Big Sky, MT, 2017b.

Conversano R, et al., "Overview of the Ascendant Sub-kW Transcelestial Electric Propulsion System (ASTRAEUS), *36th International Electric Prop. Conf.*, Vienna, Austria, Paper # IEPC-2019-282, 2019.

Harman, H. P., Rothaus, S., and Wanot, G., "µFCU - A Miniaturized Flow Control Unit for Xenon", IEPC-2013-227, October, 2013.

Hejmanowski, N. J., Woodruff, C., Burton, R.L., Carroll, D.L., and Cardin, J., "CubeSat High Impulse Propulsion System (CHIPS)," *62nd JANNAF Propulsion Meeting (7th Spacecraft Propulsion)*, Paper Tracking # 4032 (2015).

Hejmanowski N J, Woodruff C A, Burton R L, Carroll D L, Palla A D, and Cardin J M (2016), "CubeSat High Impulse Propulsion System (CHIPS) Design and Performance," *JANNAF 2016*, Paper Tracking # 4800, Phoenix, AZ, Dec 2016.

Hruby P, Demmons N, Courtney D, Tsay M, Szabo J, and Hruby V, "Overview of Busek Electric Propulsion," *36th International Electric Propulsion Conf.*, Vienna, Austria, Paper # IEPC-2019-926, 2019.

Kamhawi H, Liu T, Benavides G F, Mackey J, Server-Verhey T, Yim J, Butler-Craig N I, and Myers J, "Performance, Stability, and Thermal Characterization of a Sub-Kilowatt Hall Thruster," *36th International Electric Propulsion Conf.*, Vienna, Austria, Paper # IEPC-2019-910, 2019.

Jackson, J., et al. "13kW Advanced Electric Propulsion Flight System Development and Qualification," *35th International Electric Propulsion Conference*, Atlanta, GA. IEPC-2017-223, 2017.

Jorns, B., Gallimore, A., Hall, S., Goebel, D., Shark, S., and Welander, B., "Update on the Nested Hall Thruster Subsystem for the NextSTEP XR-100 Program", 2018 Joint Propulsion Conference, AIAA Propulsion and Energy Forum, Cincinnati, OH. AIAA 2018-4418, 2018.

Lemmer, K, "Propulsion for CubeSats," *Acta Astronautica*, 134, 231 (2017).

Lenguito G, Neff K, Barbarits J, Snyder J S, and Chaplin V, "Versatile Xenon Flow Controller for Extended Hall-Effect Thruster Power Range," *36th International Electric Propulsion Conf.*, Vienna, Austria, Paper # IEPC-2019-303, 2019.

Levchenko, I., et al., "Space micropropulsion systems for Cubesats and small satellites: From proximate targets to furthermost frontiers." *Applied Physics Reviews,* Vol. 5, 011104, 2018.

Mueller, J., "Thruster Options for Microspacecraft," AIAA Progress Series, Vol. 187, *Micropropulsion for Small Spacecraft*, M. Micci, ed., Chapter 13, p 45, 2000.

Schmidt, G., Jacobson, D., Patterson, M., Ganapathi, G., Brophy, J., and Hofer, R., "Electric Propulsion Research and Development at NASA," *6th Space Propulsion Conference*, Seville, Spain, SPC-2018-389, 2018.

Woodruff C, Parta M, Hejmanowski N, Carroll D, Su L., Gill T, Sercel C, Whittaker C, Viges E, Byrne M, and Jorns B, "Cycle Automated Mass Flow (CAMFlow) System for Hall Thrusters," *37th International Electric Propulsion Conf.*, Cambridge, MA, Paper # IEPC 2022-590, 2022.

Woodruff C A, Parta M M, Fox R T, Carroll D L, "Advanced Flow Control System for In-Space Electric Propulsion," JANNAF 2024-9660, Oklahoma City, OK, May 2024.